Korean J. Chem. Eng., 37(4), 633-640 (2020)
DOI: 10.1007/s11814-020-0486-5

pISSN: 0256-1115
eISSN: 1975-7220

Simultaneous removal of particulates and NO by the catalytic bag filter containing V_2O_5-MoO_3/TiO_2

Abdullahi Abubakar*,, Changming Li*,†, Lin Huangfu*,**, Shiqiu Gao*,**, and Jian Yu*,†**

*State Key Laboratory of Multi-phase Complex Systems, Institute of Process Engineering, Chinese Academy of Sciences, Beijing 100190, China
**School of Chemistry and Chemical Engineering, University of Chinese Academy of Sciences, Beijing 100049, China
(*Received 29 October 2019 • accepted 5 January 2020*)

Abstract−V_2O_5-MoO_3/TiO_2 based catalytic bag filters were developed for the simultaneous removal of particulates and NO in the temperature range of 200-250 °C. Good denitrification activity, dedust efficiency as well as high adhesion strength in the temperature range of 200-250 °C was exhibited. The study of catalyst powder for coating revealed that the increased V and Mo content in catalyst can elevate the low-temperature activity, and the chosen $V_{10}Mo_{10}$ sample for coating showed the best activity with 100% NO conversion at just 180 °C. The further research on catalytic bag filter found the low ratio of PTFE, high loading and long residence time (e.g., low filtration velocity or double layer filter) may help to achieve high $DeNO_x$ efficiency. The best performance was obtained with above 80% NO conversion at 200-250 °C even in the presence of SO_2/H_2O and 99.9% dust collection efficiency on the condition of 500 g/m^2 loading, 10% PTFE, 0.5 m/min filtration velocity and double layers of filter, which demonstrated great feasibility for industrial application.

Keywords: V_2O_5-MoO_3/TiO_2, Catalytic Bag Filter, $DeNO_x$, Dedusting

INTRODUCTION

The purification of low-temperature flue gas from medium/small boilers such as coking, steel and sintering to remove SO_x, NO_x and dust has been well executed in China in recent years [1-3]. To avoid the poisoning of SO_2 as well as the disadvantage of wet desulfurization (e.g., gypsum rain, white smoke plume), the process of dry desulfurization/bag-hose precipitation/low-temperature SCR of NO_x was chosen as the most popular process route for the purification of low-temperature flue gas [4,5]. SO_x was first removed with dry $NaHCO_3$ powder, the disabled desulfurizer/fly ash was then collected together by bag filter, and the NO_x was finally eliminated through honeycomb catalyst without the risk of SO_x poisoning and ash clogging. To meet the government emission standard of NO_x (<150 mg/m^3) or even ultra-low emission requirement (<50 mg/m^3) [6-8], more expensive low temperature catalyst was used with increased SCR reactor volume, and thus the low-temperature SCR unit was almost half of the cost for the total technological process [9-12]. Therefore, the development of more advanced materials and techniques will be greatly desired to lower the current project cost in industry [13-16].

The catalytic bag filter is one new kind of multifunctional bag material integrating the traditional dust collecting bag with the SCR catalyst, which can remove the NO_x and dust simultaneously with great process benefits, such as shortened process, space saving and reduced equipment investment. However, the very thin wall thickness of bag filter with short residence time may restrict the achievement of satisfactory $deNO_x$ efficiency. Several works have been done to develop Mn based catalytic systems such as MnO_x, CuMn and $MnCeNbO_x$ for coating on bag filter [17,18]. Although good catalytic efficiency was obtained in the low temperature range from 100 to 250 °C, the Mn based catalytic bag filter may easily suffer the poisoning of SO_2 [19-23]. By contrast, the V based catalyst with good anti-sulfur ability may still be a good choice for the catalytic bag filter in industry [24,25]. Owing to the much lower activity of V based catalyst at low temperature as well as the very short residence time through a catalytic bag, the V based catalytic bag filter may not have good catalytic performance and few works have been publicly reported.

Combining the as-introduced purification process of low-temperature flue gas and the properties of the catalytic bag filter, our idea is to explore the possibility for replacement of non-catalytic bag filter with V based catalytic bag filter in the current industrial process. This strategy would possess the following desirable features: 1) relieved stress of the following SCR unit with decreased usage amount of expensive honeycomb catalyst; 2) contractible technological process with decreased equipment investment; and 3) good anti-sulfur ability with long service life for V based catalytic bag filter. The catalytic bag will be of great advantage for some industrial requirements, such as the flue gas with low concentration of NO_x, deep purification of NO_x in the tail end, or limited space in a factory. The greatest challenge of the V based catalytic bag filter is how to increase its activity in the low temperature range of 200-250 °C. Our previous work developed the V_2O_5-MoO_3/TiO_2 based industrial honeycomb catalyst, which can be used at a temperature as low as 180 °C [26]. In this work, V_2O_5-MoO_3/TiO_2 based powdery catalyst with different V/Mo ratio was prepared for coating bag filter, and the effect of loading, PTFE and working condi-

†To whom correspondence should be addressed.
E-mail: cmli@ipe.ac.cn, yujian@ipe.ac.cn

tions (e.g., filtration velocity, H_2O, SO_2) on the performance of the catalytic bag filter was investigated to improve its $DeNO_x$ efficiency. Moreover, the structure of the powdery catalyst and the corresponding coated bag filter was characterized by XRD, XRF, BET, SEM and TEM to study the influence of coated catalyst particles on dust collection efficiency. The good $DeNO_x$ performance as well as dust collection efficiency manifests the promising industrial application prospect of V based catalytic bag filter.

EXPERIMENTAL SECTION

1. Catalyst and Catalytic Fabric Filter Preparation

Chemical composition of the catalyst mainly is V_2O_5, MoO_3, WO_3 and TiO_2. The powdery catalyst was prepared by mixing their metal salt precursors (NH_4VO_3, $(NH_4)_6Mo_7O_{24}{\cdot}4H_2O$, $(NH_4)_6H_2W_{12}O_{40}$) with industrial titanium dioxide. The blank bag filter, which was from Hongsheng company of China, was knitted by thin fiber glass with diameter of 5-25 μm. The ventilation property and pressure drop of the blank filter is 4.69 $cm^3/cm^2/s$ and 106 Pa, respectively. Samples were later dried at 105 °C for 4-5 hours and calcined at 450 °C for 5-6 hours. The obtained samples were finally cooled to room temperature, later crushed and sieved to powder for use. The slurry was prepared using the powdery catalyst, Polytetrafluoroethylene (PTFE) and water, and then were stirred to homogenously mix together. The PTFE was used as binder in the catalyst emulsion for coating. The catalytic particles were firmly fixed on the filter by PTFE, and nearly no particles can drop from the filter even by friction of filter with hand as shown in the Fig. S1 (supplementary). The blank filter was cut in a circular form with the size of 150 mm and subsequently immersed into the already made slurry for ten minutes. The catalytic filter was obtained after drying at 250 °C for two hours.

2. Performance Tests

The activity test of powdery catalyst was conducted in a fixed-bed quartz reactor with 650 ppm NO, 650 ppm NH_3, 3 vol% O_2, 600 ppm SO_2 (when used), 10 vol% H_2O (when used) and balanced with N_2. The catalytic activity of the fabric filter was conducted on stainless steel reactor of internal diameter of 15.5 cm. The bag filter area, filtration velocity and inflow rate were 0.018 m^2, 0.5 m/min and 7.5 L/min, respectively. The composition of feed gases includes 700 ppm NO, 700 ppm NH_3, 5 vol% O_2, 500 ppm SO_2, 10 vol% H_2O when needed and balanced with N_2. The collection efficiency of dust was tested by Hongsheng company through VDI filter material testing system from the USA. The process and method of VDI test is similar to the previous report [27]. The test condition was chosen from the built-in method of VDI: face velocity=3.3 cm/s, particle concentration=10 g/m^3, and initial pressure for deashing=5 bar. The experimental temperatures were from 180 °C to 240 °C and the process was uninterrupted until final NO value was obtained at each temperature. The inlet and outlet concentrations of gases (NO, O_2, SO_2) were examined with the online flue gas analyzer (PG250, Horiba, Kyoto, Japan). NO conversion was calculated according to the inlet and outlet concentration of NO.

$$\text{NO conversion} = \frac{[NO]_{in} - [NO]_{out}}{[NO]_{in}} \times 100\%$$

3. Characterization

X-ray fluorescence (XRF) spectrometer (AXIOS-MAX, PANalytical B.V, Holland) was used to determine the chemical composition of catalyst samples. X-ray diffraction (XRD) patterns were recorded on an X-ray diffractometer (Empyrean, PANalytical B.V, Holland) in the 2θ range of 5-90° operating at 40 KV and 40 mA using Cu Kα radiation. Nitrogen adsorption-desorption apparatus (ASAP 2020, Micromeritics Instrument Corp, USA) was used to determine the Brunauer-Emmett-Teller (BET) and Barrett-Joyner-Halenda (BJH) at 77 K. Sample masses were 0.1 g and all of them were degassed at 200 °C for 10 h prior to be measured. The microstructure and morphological study of the samples were recorded on a SU8020 scanning electron microscope (SEM, HITACHI, Japan). The particle size of catalytic slurry was characterized by a laser particle size analyzer (LS13320, Beckman Coulter, America). JEM-2100 of JEOL transmission electron microscope (TEM) at 200 kv was used.

RESULTS AND DISCUSSION

1. The Features of the Powder Catalysts for Coating

Four distinctive catalyst samples of V_2O_5-MoO_3/TiO_2 were modified in ratio of V_2O_5-MoO_3/TiO_2 (indicated as V_xMo_y) to enhance catalytic activity. Prior to the experiments, the samples were analyzed using x-ray fluorescence (XRF), and the major oxides of these samples are in Table 1 below. The content of V_2O_5 and MoO_3 with different ratio increases as it goes down the groups. The high content of active components in catalyst may increase the performance of the catalysts [10].

Fig. 1(a) displays the conversion rate of the catalyst samples with different proportion of the V_xMo_y versus the temperature of 140-280 °C. The commercial catalyst exhibited the least NO conversion rate with 18% at 140 °C and gradually increased with the rise in temperature to 95% at 240 °C, 99% at 260 °C and 99.5% at 280 °C. The increased content of V and Mo such as V_5Mo_5 resulted in the improved performance activity. MoO_3 can produce new type acid sites as well as increase the amount of acid sites to improve the $DeNO_x$ performance, as the DRIFTS and NH_3-TPD test indicated [28]. Another report also suggested that MoO_3 may improve the

Table 1. The major components of the different powdery catalysts by XRF

Samples	V_2O_5	MoO_3	WO_3	TiO_2	SiO_2	Al_2O_3	CaO
Commercial	2.36	3.15	0.52	86.24	4.65	2.89	0.21
V_5Mo_5	4.87	4.92	1.87	87.12	0.09	0.05	0.03
$V_{10}Mo_{10}$	10.32	9.86	1.67	81.09	0.08	0.07	0.01
$V_{15}Mo_{10}$	14.65	8.79	1.75	73.91	0.04	0.02	0.02

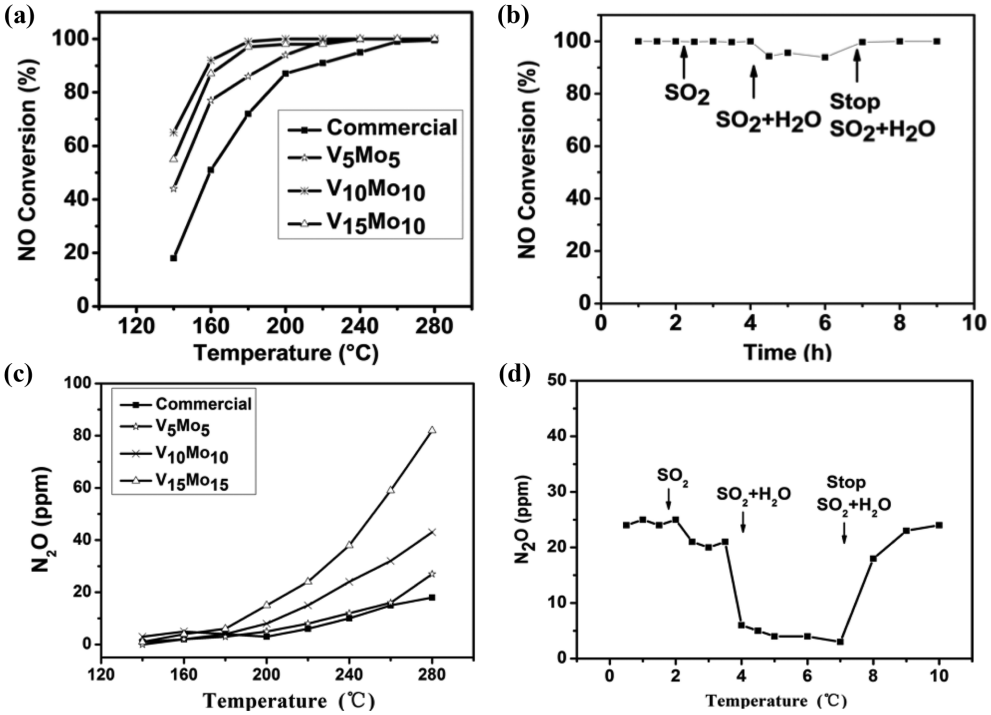

Fig. 1. The performance of powdery catalysts: different samples (a), sulfur and water resistance (b), and the formation of corresponding N_2O (c), (d).

dispersion of active components on TiO_2 [29]. The promoted effect of MoO_3 may contribute to the increased activity of V_xMo_y samples with high content of MoO_x. When the V/Mo ratio was $V_{10}Mo_{10}$, the sample demonstrated to be the best candidate of the four samples with 65% NO conversion rate at 140 °C and stabilized at 180 °C with 100% NO conversion. But the NO conversion rate declined when the V/Mo ratio was $V_{15}Mo_{10}$. The order of NO conversion rate of the examined catalyst samples is as follows: $V_{10}Mo_{10}$ >$V_{15}Mo_{10}$>V_5Mo_5>commercial catalyst. Therefore, $V_{10}Mo_{10}$ sample was chosen as the best candidate for coating the blank bag filter.

SO_2 has been a stumbling block to the successful industrialization of the selective catalytic reduction of low temperature flue gas for quite a long time, whereas the presence of water and SO_2 could lower the catalytic activity or deactivate the catalyst [30,31]. Fig. 1(b) shows the effect of water and SO_2 resistance of the selected $V_{10}Mo_{10}$ catalyst sample. To observe the effect of SO_2 on $V_{10}Mo_{10}$ catalyst sample, 500 ppm of SO_2 gas and 10 vol% H_2O were introduced into the gas stream. When SO_2 alone was earlier fed into the gas stream, changes were not observed and could be due to ability of Mo (Molybdenum) to possess sulfur resistance [25]. The production of N_2O began to increase after 200 °C for all the four samples, and the amount of the generated N_2O increased with the elevated concentration of active components in catalysts (Fig. 1(c)). Moreover, the addition of SO_2 slightly reduced the production of N_2O, but 10 vol% H_2O in synergy with SO_2 lowered the NO conversion rate to about 97% for three hours after their emergence in the gas stream. The concentration of N_2O was cut down from 20 ppm to several ppm after addition of both SO_2 and H_2O (Fig. 1D). The results demonstrate that the SO_2 and H_2O can strongly suppress the production of N_2O even over the catalysts with high content of active components [32]. Subsequently, the water and SO_2 were cut off and the conversion rate rapidly recovered and attained stability at 100% for two hours. These results indicated that the catalyst may have a very good catalytic activity and possesses SO_2 resistance ability with slight effect in the presence of SO_2 and H_2O.

2. Characterization of $V_{10}Mo_{10}$ Catalyst Sample

The powdery XRD patterns of the $V_{10}Mo_{10}$ catalyst sample are disclosed in Fig. 2(A). Only the TiO_2 anatase was able to be detected by the XRD device. In Fig. 2(A), no XRD peaks for VO_x and MoO_x were observed for $V_{10}Mo_{10}$ sample, which indicated the good dispersion of active components. Previous research found that the VO_x and MoO_x could be well dispersed on TiO_2 in the form of solid solution [33]. Fig. S1 further shows that the increased content of active components for $V_{15}Mo_{10}$ resulted in the agglomeration of catalytic particles, and its $DeNO_x$ efficiency was decreased as shown in Fig. 1. Fig. 2(B) depicts the BET details, and the observable dissimilarity in desorption/adsorption of N_2 isotherms reveals that the mesoporous were characterized by the type IV isotherms [34]. The specific surface and average pore size of the sample is 46 m^2/g and 10.5 nm, respectively. Fig. 2(C) is the SEM image representing the homogeneous dispersal of the microparticles of the sample. TEM image in Fig. 2(D) also shows the well-defined organization of the atomic particles of the sample. In addition, the SEM and TEM images for V_5Mo_5 and $V_{10}Mo_{10}$ are also shown in Fig. S2 (supplementary). It can be seen that the morphology and dispersity of V_5Mo_5 are similar to the sample of $V_{10}Mo_{10}$. But severe agglomeration is observed for $V_{15}Mo_{10}$, which may account for its non-increased activity even with its high content of active component [33].

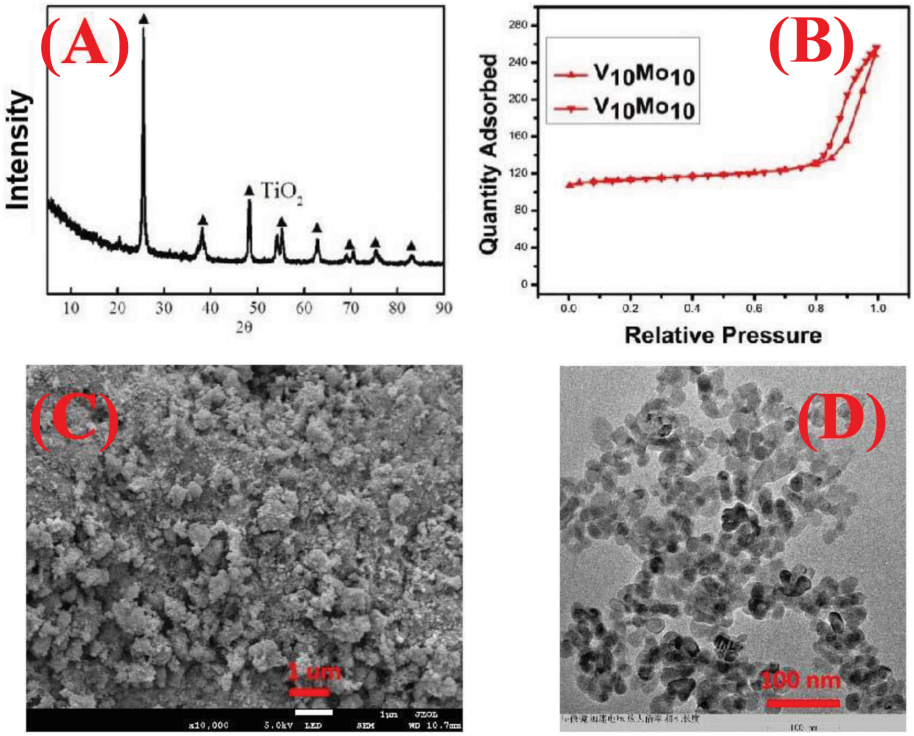

Fig. 2. The structure of the $V_{10}Mo_{10}$ sample: XRD pattern (A), N_2 adsorption-desorption isotherms curve (B), SEM image (C) and TEM image (D).

3. The Catalytic Performance of Catalytic Fiber Filter on Different Conditions

3-1. The Effect of PTFE on $V_{10}Mo_{10}$ Catalyst

PTFE (Polytetrafluoroethylene) has extraordinary strength, robustness and self-lubrication property for bag filter, which can be used for long term at maximum of 260 °C with an excellent feature as water-resistant, oil repellent and stain-resistor. It is able to fix catalyst particle size, protect against abrasion and enhance ash and particulate removal. PTFE in certain percentage is used in slurry preparation for catalytic bag filter which is later coated on the filter. And this experiment investigated the effects of PTFE on $DeNO_x$ performance for the catalytic bag filter.

Fig. 3(A) presents the catalytic fabric filter with different PTFE content from 0%, 5%, 10% and 25% PTFE under the same slurry preparation method and condition. The filter with 0% PTFE appears to be yellow, particle size was not firmly fixed, and the obtained catalytic filter was not durable, not strong, unable to resist stains and oil. Probability of falling off the catalyst from the filter is very high. In the presence of PTFE, however, the filter ability to hold particle size firmly as well as resist abrasion notably increases. The durability, water resistance, stain resistance, strength, dust and ash removal efficiency may increase with the increase of PTFE content from 0%-5%-10%-25% content.

Fig. 3(B) illustrates the catalytic activity test results of the filter samples with different content of PTFE (0%, 5%, 10% and 25%). In terms of catalytic activity test of these samples, 0% PTFE appears

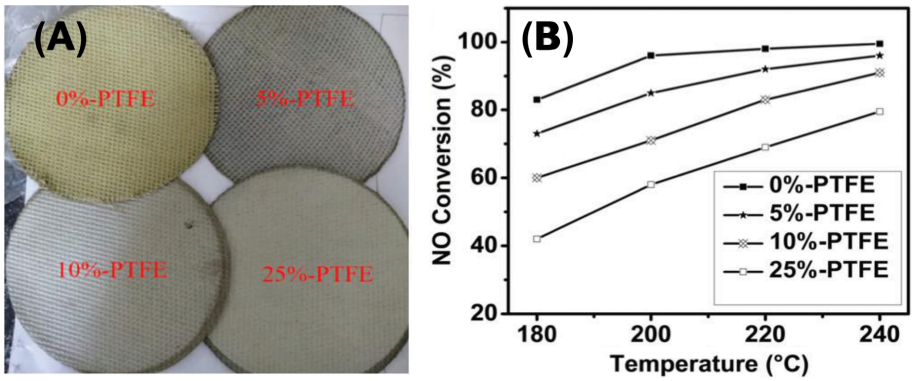

Fig. 3. The effect of PTFE on the catalytic bag filter: (A) The digital photograph photo for the samples with different PTFE; (B) The performances of the samples with different PTFE content.

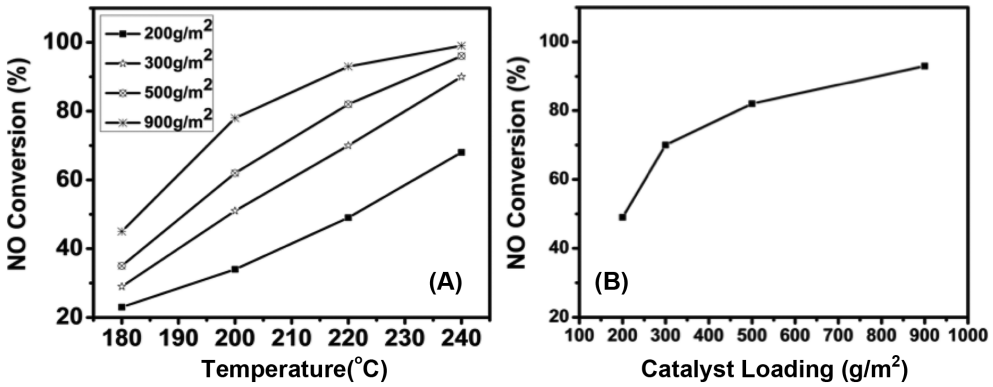

Fig. 4. The effect of catalyst loading: (A) Performance *vs* temperature; (B) performance *vs* loading at 220 °C.

to possess higher NO conversion efficiency commencing from 83% at 180 °C then up to 100% at 240 °C. Thereafter, the 5% PTFE initiated with 73% at 180 °C and 96% at 240 °C. 10% PTFE emerges to be third in performance with 60% NO conversion rate at 180 °C and finally 91% at 240 °C. Lastly, the sample with 25% PTFE only had 42% NO conversion at 180 °C and 79% NO conversion at 240 °C. It is observable that the catalytic activity of the samples was slightly lower in presence of the PTFE. The higher the PTFE content, the lower the NO removal efficiency. For better efficiency, durability and low pressure drop, the reasonable PTFE quantity exists within 5%-10% content.

3-2. The Effect of Catalyst Loading

Catalyst loading is a significant feature for NO conversion efficiency. Higher quantity of catalyst loading stimulates much more active sites for NH_3 adsorption leading to higher NO conversion [36]. As shown in Fig. 4(A), the catalytic activity of $V_{10}Mo_{10}$ catalyst sample with different catalyst loading at distinctive temperature was investigated. When the catalyst loading was 200 g/m^2, the highest conversion rate attained was 68% at 240 °C. And it can be observed to be 99% at 240 °C for catalyst loading of 900 g/m^2. Moreover, the catalytic activity increased with the increase of the temperature, possibly as a result of catalyst components activation. The chemical adsorption capability and surface energy may get stronger alongside the increment of temperatures [37]. The catalytic filter is able to perform efficiently up to 240-250 °C. Fig. 4(B) shows the catalyst loading versus the NO conversion at 220 °C, whose results indicate that the increase in catalyst loading gave rise to the increase in the denitrification performance. The graph continues to project in NO conversion rate from 200 g/m^2-900 g/m^2. Catalyst loading of 500 g/m^2 was chosen for the catalytic bag filter in this investigation because the high amount of catalyst loading increases the pressure drop, pore blockage of catalytic filter as well as high cost.

3-3. The Effect of Filtration Velocity

One of the fundamental factors for the catalytic bag filter is the filtration velocity acting in place of the gas hourly space velocity (GHSV). Fig. 5 profiles the influence of filtration velocity on catalytic bag filter. The condition is 500 g/m^2 catalyst loading of $V_{10}Mo_{10}$ sample within the range of 0.25 m/min-1.0 m/min of filtration velocity. As the filtration velocity increases, the NO conversion rate eventually decreases. The 0.25 m/min exhibited the best NO conversion efficiency of 99%, followed by 0.5 m/min with 96%, and lastly, 1.0 m/min with 81% all at 240 °C. With the increment of the reaction temperature subsequently the performance activity reached 55% at 180 °C and finally 99% at 240 °C for 0.25 m/min filtration velocity. The NO conversion efficiency of 1.0 m/min filtration velocity was 21% at 180 °C and 67% at 220 °C. The filtration velocity can alter the residence time, and high filtration velocity means a short residence time. Fig. 5 shows the changed conversion curves with different filtration velocity. It can be seen that the NO conversion decreased with the increase of filtration velocity at each temperature. The lower the filtration velocity, the lower the pressure drop and the longer the contact time between the gas and filter, resulting in the higher NO conversion. In engineering application, the filtration velocity is largely limited to not exceed 1.0 m/min [36]. Filtration velocity of 0.5 m/min was chosen for this work for better $DeNO_x$ efficiency and lower pressure drop.

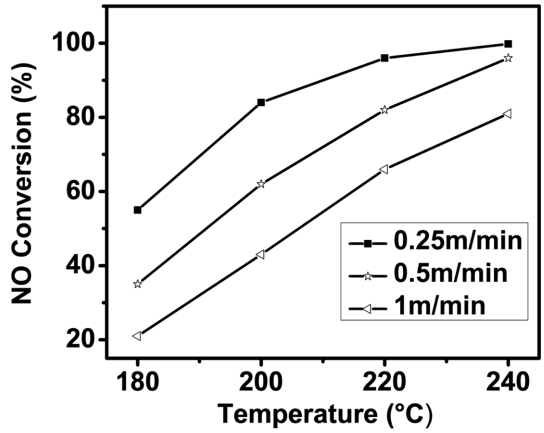

Fig. 5. The effect of filtration velocity (Standard conditions) on catalytic performance.

3-4. The Effect of Two Layer of Filter

Catalyst loading of 500 g/m^2, filtration velocity of 0.5 m/min and 10% PTFE content on $V_{10}Mo_{10}$ catalyst sample was used to investigate the effect of single layer, double layer catalytic filter activity with its resistance to SO_2 and H_2O. The double layers of filter may increase the residence time of SCR reaction for better $DeNO_x$ efficiency. Fig. 6(A) shows the NO conversion rate versus

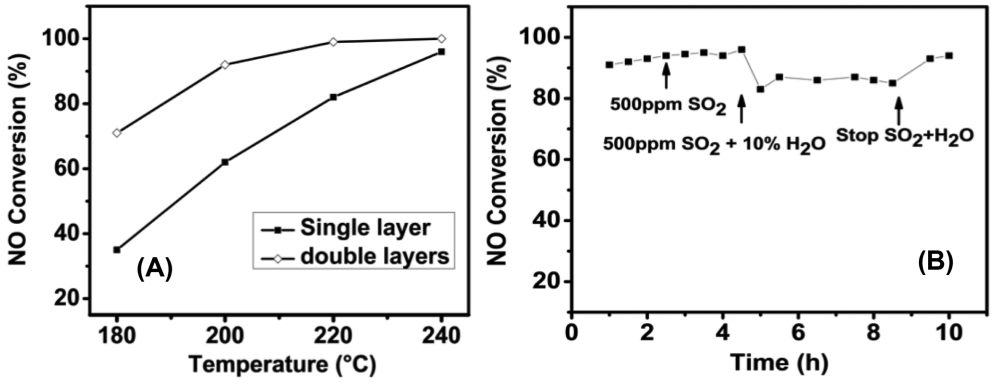

Fig. 6. The effect of different layer of catalytic bag filter (A) as well as SO_2/H_2O (B) on the catalytic performance.

temperature for single and double filter layers. The single layer NO conversion efficiency was 35% at 180 °C and gradually increased with the rise in temperature to 96% NO conversion at 240 °C. Improvement in the side of the double layer catalytic filter was observed with the conversion rate reaching 71% at 180 °C and higher progress with the rise in temperature to 100% at 240 °C. SO_2 and 10 vol% H_2O resistance tests are shown in Fig. 6(B). Prior to SO_2 introduction into the gas stream, NO conversion efficiency was observed to be about 91% from the first and second hour. But following 500 ppm of SO_2 participation into the gas stream, the conversion rate slightly projected above 92% for two hours. At the fifth hour, H_2O was released in synergy with SO_2 into the gas stream, then subsequently a decline in the NO conversion was observed, which could be due to struggle in adsorption between SO_2 and H_2O [5]. When SO_2 and H_2O were terminated, the performance immediately improved, possibly due to Mo reducing SO_2 adsorption [38]. The double layer filter obviously passed the single layer in NO conversion efficiency and it also possessed a good resistance to SO_2 and slight effect in SO_2 and H_2O synergic partake. The demonstrated high $DeNO_x$ efficiency as well as good resistance to SO_2 and water implied its promising prospect in industry.

4. The Structure and Dust Removal Performance of Catalytic Filter

SEM image in Fig. 7(A)-(B) shows the magnification images of the bag filter in diverse magnification. Fig. 7(A) presents an image of the blank filter without catalyst coating, and the fabric like structure can be clearly visible. Fig. 7(B) gives a closer magnification image showing the uniform distribution of fabric with the pore of several micrometers. The filter loaded with catalyst is displayed in Fig. 7(C) and the magnified one in Fig. 7(D). It can be seen for the

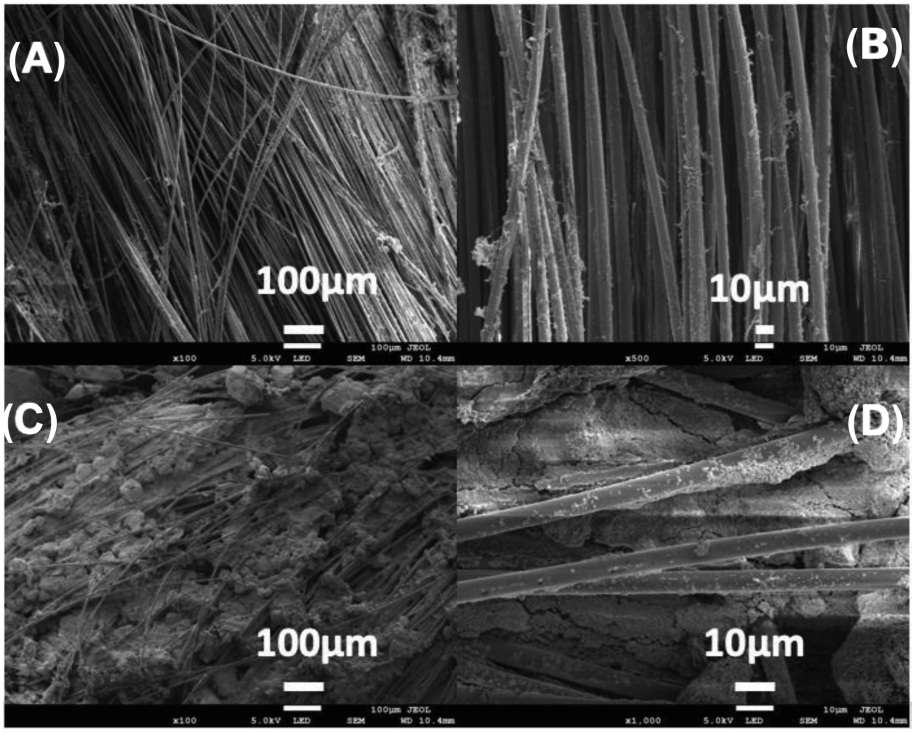

Fig. 7. SEM images of the blank filter (A), (B) and the catalyst bag filter (C), (D) with different magnification times.

Table 2. The VDI test results for different bag filter samples

Samples	Ventilation property ($cm^3/cm^2/s$)	Pressure drop (Pa)	Dust removal efficiency
Blank filter	4.69	106	99.9%
Catalyst filter (300 g/m^2)	3.76	189	99.9%
Catalyst filter (500 g/m^2)	2.53	236	99.9%
Catalyst filter (1,000 g/m^2)	1.67	589	99.9%

filter with loading of 500 g/m^2 that the space among filters was filled with catalyst particles. The size of pore decreased, which may increase the pressure drop of the catalytic bag filter.

For the dust removal efficiency of the catalytic filters, VDI test of the catalytic filter was executed. The results are displayed in Table 2 for the $V_{10}Mo_{10}$ sample with different catalyst loading. As shown in the results, the ventilation property decreased with the increase of catalyst loading. Correspondingly, the pressure drop notably increased. All the filters achieved the dust removal efficiency of 99.9% which meets the membrane filter standard [37]. In industry, the ventilation property should be higher than 2.5 $cm^3/cm^2/s$, and the pressure drop should be lower than 250 Pa. Thus, the catalytic loading should be lower than 500 g/m^2. Combining the above active results, the catalytic filter with 10% PTFE and 500 g/m^2 loading can achieve up to above 80% $DeNO_x$ efficiency as well as 99.9% dust removal efficiency on the condition of 220 °C and 0.5 m/min. Moreover, the double layer of filter can even have good SO_2/H_2O-resistance with much higher $DeNO_x$ efficiency of above 90% at 220 °C, which shows promising prospect in industry.

CONCLUSION

V_2O_5-MoO_3/TiO_2 based catalytic bag filters were prepared through coating the corresponding catalytic slurry, which demonstrated good $DeNO_x$ efficiency from 60% to 90% in the temperature range of 200-250 °C, 99.9% dust collection efficiency and good adhesion strength. The study of the powdery catalysts indicated that the active V and Mo components were well dispersed on TiO_2 support with small and uniform particle size, and the increased V and Mo content helped to achieve high $DeNO_x$ efficiency, especially for the sample of $V_{10}Mo_{10}$ with 100% NO conversion at just 180 °C. After coating the catalytic slurry of $V_{10}Mo_{10}$, it was found that both the decreased content of PTFE in slurry and elevated catalytic loading may promote the performance of catalytic bag filter. On the other hand, the low content of PTFE may weaken the adhesion strength of particles on filter, and the high loading may increase the drop pressure. Moreover, the decreased filtration velocity and using two layers of filter also observably increased the $DeNO_x$ performance with much longer residence time. The best $DeNO_x$ efficiency can be achieved up to above 80% in the temperature range of 200-250 °C even in the presence of SO_2/H_2O on the condition of 500 g/m^2 loading, 10% PTFE, 0.5 m/min filtration velocity and double layers of filter. The structural characterization of filter showed that the catalytic particles uniformly filled in the interspace of cellosilks with 99.9% collection efficiency. The good $DeNO_x$ and dedusting performance of the as-prepared V_2O_5-MoO_3/TiO_2 based catalytic bag filter may have a promising prospect in industry and its further pilot plant test is under way in a coking plant.

ACKNOWLEDGEMENTS

The authors are grateful for the financial support of the International Science and Technology Cooperation Program of China (2016YFE0128300), National Natural Science Foundation of China (Grant 21601192 and 21878310), and the independent subject from State Key Laboratory of Multi-phase Complex Systems (Grant MPCS-2019-0-03). We also appreciate Zhejiang Hongsheng Environmental Technology Group Co., Ltd for their technical support of filter bag by Lixin Shen, Jun Cui and Li Gang.

REFRENCES

1. C. Li, Y. Jian, Y. He, P. Li, C. Wang, F. Huang and S. Gao, *RSC Adv.*, **8**, 18265 (2018).
2. S. Zhang, B. Zhang, B. Liu and S. Sun, *RSC Adv.*, **7**, 26226 (2017).
3. X. Yao, T. Kong, S. Yu, L. Li, F. Yang and L. Dong, *Appl. Surf. Sci.*, **402**, 208 (2017).
4. M. Zhang, B. Huang, H. Jiang and Y. Chen, *Chin. J. Chem. Eng.*, **25**, 1695 (2017).
5. L. Lietti, I. Nova and P. Forzatti, *Top. Catal.*, **12**, 111 (2000).
6. Y. Shi, Y. F. Xia, B. H. Lu, N. Liu, L. Zhang, S. J. Li and W. Li, *Appl. Phys. Eng.*, **15**, 454 (2014).
7. H. Yang, Y. Zhang, C. Zheng, X. Wu, L. Chen, J. S. Fu and X. Gao, *Energy*, **161**, 523 (2018).
8. http://zfxxgk.nea.gov.cn/auto84/201608/t20160804_2283.htm.
9. R. Dvořák, P. Chlápek, D. Jecha, R. Puchýř and P. Stehlík, *J. Clean. Prod.*, **18**, 881 (2010).
10. Z. Ma, X. Wu, Y. Feng, Z. Si, D. Weng and L. Shi, *Prog. Nat. Sci. Mater. Int.*, **25**, 342 (2015).
11. A. Marberger, D. Ferri, D. Rentsch, F. Krumeich, M. Elsener and O. Kröcher, *Catal. Today*, **320**, 123 (2017).
12. I. Song, S. Youn, H. Lee, S. G. Lee, C. J. Cho and D. H. Kim, *Appl. Catal. B Environ.*, **210**, 421 (2017).
13. S. M. Mousavi, *Chin. J. Chem. Eng.*, **24**, 914 (2016).
14. L. Zhu, Z. Zhong, J. Xue, Y. Xu, C. Wang and L. Wang, *J. Environ. Sci. (China)*, **65**, 306 (2018).
15. M. Aguilar-romero, R. Camposeco, S. Castillo, J. Marin, V. Rodríguez-González, L. A. García-Serrano and I. Mejía-Centeno, *Fuel*, **198**, 123 (2017).
16. T. Xu, X. Wu, Y. Gao, Q. Lin, J. Hu and D. Weng, *Catal. Commun.*, **93**, 33 (2017).
17. Y. S. Zhang, C. Li, C. Yu, T. Tran, F. Guo, Y. Yang, J. Yu and G. Xu, *Chem. Eng. J.*, **330**, 1082 (2017).
18. M. Kang, E. D. Park, J. M. Kim and J. E. Yie, *Korean J. Chem. Eng.*,

26, 86 (2009).
19. S. Zhang and Q. Zhong, *J. Mol. Catal. A: Chem.*, **373**, 108 (2013).
20. H. Chang, J. Li, J. Yuan, L. Chen, Y. Dai, H. Arandiyan, J. Xu and J. Hao, *Catal. Today*, **201**, 139 (2013).
21. R. Jin, Y. Liu, Z. Wu, H. Wang and T. Gu, *Catal. Today*, **153**, 84 (2010).
22. J. Yu, F. Guo, Y. Wang, J. Zhu, Y. Liu, F. Su, S. Gao and G. Xu, *Appl. Catal. B-Environ.*, **95**, 160 (2010).
23. S. Yu, Y. Lu, Y. Cao, Y. Wang, B. Sun, F. Gao, C. Tang and L. Dong, *Catal. Today*, **327**, 235 (2019).
24. H. Chang, J. Li, W. Su, Y. Shao and J. Hao, *Chem. Commun.*, **50**, 10031 (2014).
25. Y. Xu, X. Wu, Q. Lin, J. Hu, R. Ran and D. Weng, *Appl. Catal. A Gen.*, **570**, 42 (2019).
26. J. Yu, C. Li, F. Guo, S. Gao, Z. Zhang and K. Matsuoka, *Fuel*, **219**, 37 (2018).
27. J. Binnig, J. Meyer and G. Kasper, *Powder Technol.*, **189**, 108 (2009).
28. L. Zhu, Z. Zhong, H. Yang and C. Wang, *J. Environ. Sci. (China)*, **56**, 169 (2017).
29. Y. Qiu, B. Liu, J. Du, Q. Tang, Z. Liu, R. Liu and C. Tao, *Chem. Eng. J.*, **294**, 264 (2016).
30. X. Huang, S. Zhang, H. Chen and Q. Zhong, *J. Mol. Struct.*, **1098**, 289 (2015).
31. Q. Zhang, C. Song, G. Lv, F. Bin, H. Pang and J. Song, *J. Ind. Eng. Chem.*, **24**, 79 (2015).
32. B. Zhang, M. Liebao, W. Suprun, B. Liu, S. Zhang and R. Gläser, *Catal. Sci. Technol.*, **9**, 4759 (2019).
33. L. Han, S. Cai, M. Gao, J. Y. Hasegaya, P. Wang, J. Zhang, L. Shi and D. Zhang, *Chem. Rev.*, **119**, 10916 (2019).
34. T. S. Tran, J. Yu, C. Li, F. Guo, Y. Zhang and G. Xu, *RSC Adv.*, **7**, 18108 (2017).
35. C. Chen, Y. Cao, S. Liu, J. Chen and W. Jia, *CuihuaXuebao/Chinese J. Catal.*, **39**, 1347 (2017).
36. B. Yang, Y. Shen, Y. Su, P. Li, Y. Zeng and S. Shen, *J. Ind. Eng. Chem.*, **50**, 133 (2017).
37. B. Yang, D. H. Zheng, Y. S. Sheng, Y. S. Qiu, B. Li and Y. W. Zeng, *J. Ind. Eng. Chem.*, **24**, 148 (2015).
38. D. W. Kwon, K. H. Park and S. C. Hong, *Chem. Eng. J.*, **284**, 315 (2016).